

Microphysical Scaling Relations in a Kinematic Model of Isolated Shallow Cumulus Clouds

AXEL SEIFERT

Deutscher Wetterdienst, Offenbach, Germany

BJORN STEVENS

Max-Planck-Institut für Meteorologie, Hamburg, Germany, and Department of Atmospheric and Oceanic Sciences, University of California, Los Angeles, Los Angeles, California

(Manuscript received 14 September 2009, in final form 11 December 2009)

ABSTRACT

The rain formation in shallow cumulus clouds by condensational growth and collision–coalescence of liquid drops is revisited with the aim of understanding the controls on precipitation efficiency for idealized cloud drafts. For the purposes of this analysis, a one-dimensional kinematic cloud model is introduced, which permits the efficient exploration of many microphysical aspects of liquid shallow clouds with both spectral and two-moment bulk microphysical formulations. Based on the one-dimensional model and the insights gained from both microphysical approaches, scaling relations are derived that provide a link between microphysical and macroscopic cloud properties. By introducing the concept of a macroscopic autoconversion time scale, the rain formation can be traced back to quantities such as cloud depth, average vertical velocity, lapse rate, and cloud lifetime. The one-dimensional model also suggests that the precipitation efficiency can be expressed as a function of the ratio of the macroscopic autoconversion time scale and cloud lifetime and that it exhibits threshold-like behavior.

1. Introduction

Attempts to rationalize rain formation, even for relatively simple, shallow cumulus clouds, is frustrated by the range of scales encompassed by the processes involved, and the complexities of the interactions between the fluid-thermodynamical and particle-kinetic processes. The past years have seen many important advances in our attempts to work our way through the scales and processes involved. By extending the classical work of von Smoluchowski (1916, 1917) and Müller (1928) to a fully probabilistic formulation, the derivation of the quasi-stochastic collection equation (SCE) by Gillespie (1972) is one of the landmark achievements in the entire field of parameterization of atmospheric processes, forming the starting point for theoretical studies of warm rain microphysics. Although the development of the theory of quasi-stochastic collection enormously reduces the degrees of freedom in cloud

microphysical parameterization, it requires a detailed representation of the distribution of cloud drops. Subsequent work, starting from the SCE, has addressed this limitation by attempting to reproduce the essential behavior of particle kinetic interactions in terms of parametric representations of the cloud drop distribution. The resulting models, often called bulk-microphysical models, have met with some degree of success (e.g., Berry and Reinhardt 1974; Clark 1974; Lüpkes et al. 1989; Beheng 1994; Reisner et al. 1998; Khairoutdinov and Kogan 2000; Seifert and Beheng 2001, hereafter SB01; Milbrandt and Yau 2005a,b; Morrison and Grabowski 2007, hereafter MG07). Even so, such schemes are applicable on scales where the drop size distribution can be expected to be relatively homogeneous, which is necessarily much smaller than the scale of individual clouds.

Perhaps for a lack of a better idea, the bulk microphysical concepts developed for individual cloud parcels have been used to model the microphysical evolution of clouds as a whole (Kessler 1969), or even fields of clouds, (e.g., Lohmann and Roeckner 1996) in which case many of the parameters of the model lose their physical

Corresponding author address: Dr. Axel Seifert, Deutscher Wetterdienst, Frankfurterstr. 135, 63067 Offenbach, Germany.
E-mail: axel.seifert@dwd.de

meaning (Rotstajn 2000), or the basic structure of the model may be changed. Naturally many questions and controversies arise. For instance, Kessler's influential parameterization treats rain formation as a threshold process that is insensitive to drop number. Such an approach has been widely criticized as on the scale of homogeneous cloud parcels we know that the collision kernel is nonzero for disperse droplet distributions; that is, from a purely microphysical point of view all clouds would develop precipitation-sized particles sooner or later (cf. SB01). Moreover, parameterizations of rain formation based on the SCE, as well as solutions of the SCE itself, show a robust sensitivity to droplet number concentration, which is often not evident in the threshold or Kessler-like models (Beheng and Doms 1986). But how relevant are the ideas developed on the scale of homogeneous cloud parcels to the macroscopic (cloud scale) evolution of cloud microphysical processes? Indeed, what is the role of the cloud dynamical processes in determining its microphysical evolution?

These questions form the backdrop of the present study, where we develop a simple framework for exploring the interplay between dynamic and microphysical processes in the evolution of a cloud as a whole. So doing provides an opportunity to evaluate cloud-microphysical models anew, in a somewhat more dynamic context, as well as to explore bulk relationships that may emerge on the scale of individual clouds or cloud drafts.

Our approach is to use a hierarchy of microphysical models in a simplified (kinematic) dynamical framework. The microphysical models range from a discretized form of the spectral formulation, the bin microphysics model, to a two-moment bulk scheme. The latter helps to identify key parameters to include in subsequent theoretical investigations of the precipitation efficiency of macroscopic clouds. The dynamic framework is highly idealized, and kinematic, but isolates what we believe to be essential cloud macrophysical parameters, these being the lapse rate of cloud water, the cloud updraft speed, and the cloud lifetime. It is motivated by our earlier analyses of high-resolution simulations of precipitation development in shallow cumulus convection (Stevens and Seifert 2008), as well as a recent study of the life cycle of shallow cumulus (Heus et al. 2009).

Ultimately our aim is not so much to suggest yet another parameterization—although in the end the results can be used in that way—but to provide some understanding of the involved processes and their importance for aerosol–cloud–precipitation interaction. Nor do we wish to claim that our simple kinematic framework encompasses all of the essential processes determining the formation of rain in shallow cumulus clouds, let alone

other forms of convection. Rather, it provides a useful starting point for furthering the development of our theoretical understanding of the ways in which cloud microphysical and macrophysical processes interact.

The remainder of the paper is organized as follows: in section 2 we will introduce the 1D kinematic cloud model used in this study, including some details on activation of cloud condensation nuclei (CCN) and condensational growth of droplets. In section 3 some results of the numerical simulations of the bin and two-moment bulk scheme are discussed, and the dataset used in the rest of the paper is introduced. In section 4 the principal sensitivities of the kinematic model are explored, and yet simpler models are derived that capture these relationships, including a new parameterization of bulk activation of CCN, a relationship for the macroscopic auto conversion time scale as measure of the time needed for rain formation in a cloud, and the processes determining the rate of precipitation formation and the precipitation efficiency of shallow cumulus clouds. The paper closes with a summary, conclusions, and an outlook in section 5.

2. An idealized 1D kinematic cloud model

To investigate the precipitation formation in shallow convective clouds, we use an idealized 1D warm rain cloud model. This model explores the evolution of the size spectrum of liquid water within a single vertical column and for a prescribed flow. Essentially, we propose that an extension of a 1D rain shaft model can provide useful insight into choices one must make in the formulation of microphysical processes, on one hand, and a framework for developing new, aggregate models more appropriate to the cloud scale, on the other.

Let $f(x, z, t)$ denote the number density of water drops so that $f(x, z, t) dx$ is the number of drops per cubic meter in the mass interval $[x, x + dx]$ at some height z and time t . It follows that the liquid-water mixing ratio is

$$q_l(z, t) = \rho_0^{-1} \int_0^{\infty} x f(x, z, t) dx, \quad (1)$$

where ρ_0 denotes the ambient density of the two-fluid (water and dry air) system in which the liquid drops are suspended. Because the clouds that we attempt to model are assumed to be much shallower than an atmospheric scale height, we fix ρ_0 as constant with a value of 1.065 kg m^{-3} .

In one spatial dimension, neglecting the direct effects of lateral mixing, the evolution of f may be described as follows:

$$\frac{\partial f}{\partial t} + \frac{\partial}{\partial z} [(w + v(x))f] + \frac{\partial}{\partial x} \left[\frac{dx}{dt} f \right] = \mathcal{S}(s, f) + \mathcal{K}(f). \tag{2}$$

On the lhs, the second term describes the motion of drops in the vertical and comprises two components: $v(x)$ denotes the terminal settling velocity and is prescribed as a function of mass only, following Beard (1976); $w(z, t)$ denotes the ambient flow. The third term describes the effects of vapor diffusion to or from existing drops. On the rhs, \mathcal{S} describes the creation or destruction of cloud droplets due to the activation of cloud condensation nuclei or the total evaporation of a droplet; it depends on the supersaturation s and f . The last term denotes kinetic (collision, coalescence, and breakup) effects [see Seifert et al. (2005) for details on the collision terms]; because \mathcal{K} is known, given f , closure of (2) requires the prediction of the supersaturation s and the growth rate dx/dt (itself a function of s) given an ambient flow, $w(z, t)$.

a. The cloud model

Vapor diffusion depends on the growth rate of individual drops, which to a good degree of approximation can be written as

$$\frac{dx}{dt} = 4\pi r G(T, p) f_v(r) s \tag{3}$$

with r denoting the drop radius. The principal thermodynamic dependence is carried by the supersaturation $s = e/e_s - 1$, where e is the vapor pressure and e_s its saturation value. The weak dependence of the growth rate on the thermodynamic state is encapsulated by

$$G(T, p) = \left(\frac{R_v T}{D_v e_s(T)} + \frac{L_v^2}{\kappa_a R_v T^2} \right)^{-1}, \tag{4}$$

with D_v the diffusivity of water vapor in air, R_v the gas constant of water vapor, L_v the enthalpy of vaporization of water, κ_a the diffusivity of heat in air, T the temperature, and p the pressure. For completeness (3) includes ventilation effects through the coefficient $f_v(r)$, which, when important, are prescribed following Pruppacher and Klett (1997). The above implies that, given a drop distribution, dx/dt and s are determined given T , q_v , and p .

Rather than solve prognostic equations for each of these thermodynamic quantities, we introduce a simplified representation of the thermodynamics, which we believe captures the essential aspects of the evolution of a developing cloud. Our formulation requires only one

additional prognostic equation, that for the *adiabatic* specific humidity, $\tilde{q}_v(z, t)$, where

$$\frac{\partial \rho_0 \tilde{q}_v}{\partial t} + \frac{\partial}{\partial z} (w \rho_0 \tilde{q}_v) + \int_0^\infty \frac{dx}{dt} f dx = 0. \tag{5}$$

Mixing is measured by a diabatic deviation, q'_v , such that the actual specific humidity of a rising parcel is simply $q_v = \tilde{q}_v + q'_v$. We expect q'_v , which measures the desiccation of an air parcel due to mixing with the environment, to be negative. Because $e/e_s \simeq q_v/q_s$, we can write

$$s = \frac{\tilde{q}_v}{q_s(T_*, p)} - 1 \tag{6}$$

if the effective temperature T_* is defined such that $q_s(T_*, p) = q_s(T, p) \tilde{q}_v/q_v$. Because differences between T and T_* are on the order of a percent or two, $G(T, p) \approx G(T_*, p)$. A closed representation of these terms thus requires a prescription of T_* and p .

To solve for T_* we assume that moist enthalpy differences between the cloud and its environment scale with moisture differences, in which case

$$T_* \simeq \tilde{T} - q'_v \left(\frac{R_v \tilde{T}^2}{q_s L_v} \right) \left(1 + \frac{L_v^2 q_s}{R_v c_p T^2} \right)^{-1}, \tag{7}$$

where \tilde{T} is the adiabatic temperature. Considering $q'_v < 0$, corresponding to clouds mixing with a drier environment, one expects T_* to be greater than \tilde{T} , even though $T < \tilde{T}$. This emphasizes that T_* is not the actual cloud temperature but rather the temperature required to predict the correct supersaturation given that \tilde{q}_v is the adiabatic, as opposed to the actual, specific humidity. Equation (7) suggests that to a first approximation simply specifying T_* as a function of height can serve to parameterize cloud updrafts that progressively mix as they rise. Hence, in our subsequent investigations we close our model by specifying

$$T_* = T_b + \Gamma_*(z - z_b), \tag{8}$$

where T_b is the temperature at cloud base, whose height we measure by z_b , and fix p with a hydrostatic profile. We expect $\Gamma_m > \Gamma_* > 0$, with Γ_m denoting the moist adiabatic lapse rate. From this model it follows that in the absence of droplet growth by collision-coalescence, the equilibrium cloud water content in the absence of collision-coalescence processes is simply $\rho_0 c_p / L_v \Gamma_*(z - z_b)$.

The purpose of formulating our model in terms of \tilde{q}_v and T_* is to encapsulate the effects of mixing, and hence the tendency of clouds to be subadiabatic, in a single

parameter, Γ_* . So doing results in a simple model capable of producing clouds whose liquid water content increases at some fraction of the adiabatic rate under the influence of a realistically evolving supersaturation field.

Even as a kinematic framework the model has some shortcomings. It decouples the temperature field from the degree of sub- or supersaturation. In real clouds more rapid ascent, or reduced CCN concentrations, can be expected to produce greater supersaturation, which implies less condensational warming although, because supersaturation differences are not large, this effect will be modest. It also is valid only for a restricted set of mixing scenarios, namely those in which the net mixing (dilution) depends only on the displacement of a parcel and for which the cloud-environment temperature differences scale with differences in the specific humidity. Moreover, as implemented, our model assumes that mixing is homogeneous in that the full population of drops at each point responds to the thermodynamic environment at that point. Finally, many of the rationalizations work best for small perturbations, which means the model is most appropriate for shallow clouds.

b. Activation of CCN

The activation process is calculated using the resolved supersaturation given a parameterization of the Köhler theory. We follow the approach of MG07, which in turn is based on Khvorostyanov and Curry (2006, hereafter KC06); see also von der Emde and Wacker (1993) and Ghan et al. (1993) for related and earlier work. The basic approach assumes that the dry aerosol can be well described by a lognormal distribution [Eq. (4) of KC06] and represents the activation rate as

$$\left. \frac{\partial N_c}{\partial t} \right|_{\text{nuc}} = \max\left(\frac{N_{\text{ccn}} - N_c}{\Delta t}, 0\right), \quad (9)$$

where Δt is the long (advective) time step and

$$N_{\text{ccn}} = N_a \frac{(s/s_0)^{k_0}}{1 + (s/s_0)^{k_0}} \quad (10)$$

is the number of CCN that would be expected to activate at the supersaturation s . The coefficients k_0 and s_0 encode the physiochemical properties of the aerosol, with

$$s_0 = r_{a,d}^{-(1+\beta_a)} \left(\frac{4A_k^3}{27b_d}\right)^{1/2}; \quad k_0 = \frac{4}{\sqrt{2\pi}(1+\beta_a)\ln\sigma_{a,d}}. \quad (11)$$

Here, the shape of the assumed dry aerosol distribution is represented by its number concentration N_a , its geometric

mean radius $r_{a,d}$, and the dispersion $\sigma_{a,d}$. In what follows N_a is varied while $r_{a,d}$ and $\sigma_{a,d}$ are fixed at $0.485 \mu\text{m}$ and 2. The chemical properties are given by the parameters b_d and β_a , which we fix at 0.25 and 0.5, respectively, meaning the soluble fraction is distributed within the particle, not on the surface (see KC06 for details). Finally, A_k denotes the Kelvin curvature parameter, whose value is fixed at 1.08 nm.

c. Bulk versus bin models

What we call the bin model is a solution of Eq. (2) given a nonparametric representation of f ; that is, it is discretized over its dependent variables (x, z, t) subject to the evolution of the temperature and moisture fields as discussed above. The bulk model assumes that f conforms to a distribution of some assumed form over x and thus specifies its evolution through the evolution of some small number of moments (or parameters) of that distribution. The bulk model we explore is based on SB01 with modifications following Stevens and Seifert (2008) and as otherwise noted. Both schemes use the same activation parameterization, with the additional assumption that activated drops have a radius of $1 \mu\text{m}$ (smallest size bin) in the bin scheme. Both also use the same parameterization of sedimentation and an explicit condensation scheme.

For the bin microphysics condensation [term 3 of Eq. (2)] is solved using a first-order upwind scheme. To ensure numerical stability a time-splitting procedure is used with a substep below 1 s. Using a first-order upwind scheme introduces a considerable amount of artificial diffusion. However, because we neglect the effects of small-scale mixing on the evolution of the droplet spectrum, such numerical diffusion may not be as deleterious as might otherwise be expected. Nonetheless, a better treatment of the condensation—for instance, following the method of Brenguier (1991)—and an explicit treatment of small-scale mixing would represent an improvement on the present approach.

For the two-moment bulk microphysics a simplified vapor diffusion term can be derived by integrating the size-dependent condensation rate (3) over the size spectrum (see also MG07). So doing results in a bulk condensation rate that can be written as

$$\left. \frac{\partial q_c}{\partial t} \right|_{\text{cond}} = 4\pi\rho_0^{-1}N_c\bar{r}_cGs \cong \frac{\tilde{q}_v - q_s}{\tau_c}. \quad (12)$$

Here subscript c denotes the cloud droplet portion of the liquid water spectrum. The parameter τ_c denotes the condensation time scale for cloud droplets and follows from integrating (3) and (4), which for $s \ll 1$ yields

$$\tau_c = (4\pi D_v N_c \bar{r}_c)^{-1}, \quad (13)$$

where N_c is the number concentration of cloud droplets and

$$\bar{r}_c = \frac{1}{N_c} \int_0^\infty r f_c(x) dx \quad (14)$$

is the geometric mean radius of cloud droplets, with f_c the cloud droplet number distribution. Because ventilation effects for cloud droplets are negligible, this effect has not been accounted for in our derivation of τ_c , although to do so would be straightforward.

Assuming a gamma distribution over mass, as in SB01—that is, $f_c(x) = Ax^\nu \exp(-\lambda x)$ —we find

$$\bar{r}_c = \alpha_{rc} \frac{\Gamma(\nu + 4/3)}{\Gamma(\nu + 1)} \left[\frac{3}{4\pi\rho_w} \frac{q_c}{(\nu + 2)N_c} \right]^{1/3}, \quad (15)$$

where q_c is the cloud water content, ρ_w the density of liquid water, and Γ the gamma function. We introduced α_{rc} as a tuning factor since the assumption of a gamma distribution and especially the chosen value of ν might not be appropriate near cloud base where the condensation time scale is decisive for the activation process. In the following we chose $\nu = 3$ because it conforms best to the width of the drop distribution of the spectral model. Subsequently, the tuning factor was adjusted to $\alpha_{rc} = 0.3$ to match the supersaturation and cloud droplet number concentration of the bin model. The value of 0.3 of this tuning factor could, for example, be explained with a somewhat narrower droplet distribution with $\nu = 5$.

The treatment of evaporation of rain drops is identical to Seifert (2008); for example, ventilation effects are included in the bin and the bulk model. Lastly, we note that for the raindrop spectrum the parameterization of the shape of the distribution in terms of its mean volume radius follows the proposal by Seifert (2008) with the minor modification of a continuous transition between in-cloud and below-cloud assumptions.

d. Initial data and velocity profile

For the initial data we assume a cloud base with relative humidity $\text{RH} = 100\%$ at 500-m height at a pressure of 950 hPa. Below cloud base the boundary layer is well mixed with a potential temperature of $\theta_0 = 297.2$ K and \tilde{q}_v initially constant at some specified value. Above the boundary layer, \tilde{q}_v is set low enough to ensure that a secondary cloud does not develop at upper levels as long as this condition is satisfied (e.g., by setting $\tilde{q}_v = 0$ above z_b ; the initial profile of \tilde{q}_v above cloud base plays no role in the model), and the environmental humidity is implicitly specified through T_* .

We specify the vertical velocity to be constant with height, such that

$$w(z, t) = w(t) = w_0 \sin\left(\frac{2\pi t}{\tau_w}\right), \quad (16)$$

where $w \geq 0$ leads to the growth of a saturated layer above cloud base. Specifying w to be independent of height is a bit unrealistic as velocities are well known to initially increase with height in clouds (and then decrease again near cloud top). However, so doing focuses our analysis on the temporal development of the cloud and at least captures the tendency of the leading edge to accelerate as it deepens. We need not make this assumption but do so to help limit the principal parameters to three (Γ_* , w_0 , and τ_w) and avoid the problem of having to make explicit statements about the nature of entrainment and mixing—consistent with our simplified thermodynamic treatment of these processes.

3. Numerical experiments

In this section we explore the behavior of the kinematic cloud model with a particular focus on the ability of the bulk microphysical model to reproduce the principal features evident in simulations based on the bin model. Our kinematic cloud model was formulated to isolate what we believe to be essential control parameters—namely the in-cloud lapse rate Γ_* ; the maximum updraft speed w_0 ; the cloud lifetime τ_w , and the ambient CCN. Although the model identifies a number of other parameters such as the cloud-base height, surface temperature, physiochemical properties of the aerosol, etc., these are considered secondary and are held fixed in what follows.

Notwithstanding the idealizations, the model appears to capture many features of real shallow cumulus clouds, at least insofar as high-resolution large-eddy simulations may be taken as a reference (cf. Stevens and Seifert 2008). This is evident in either column of panels in Figs. 1 and 2, which present time–height diagrams detailing the evolution of various fields. For our choice of control parameters the liquid water content reaches about 1.5 g m^{-3} . The first rain forms in the uppermost part of the cloud, about 20 min after the cloud first forms, and collects much of the cloud water during its fallout through an active rain phase of about 10 min. A thin layer of cloud lingers above the region where the rain begins to form. Within the rain shaft, size sorting is evident with the largest drops reaching the surface first, with the mean volume diameter of the raindrops approaching 0.7 mm. Activation of cloud drops occurs only at cloud base and the activated fraction is about 50% at a maximum supersaturation of 0.4%. Due to growth by condensation the mean volume diameter of

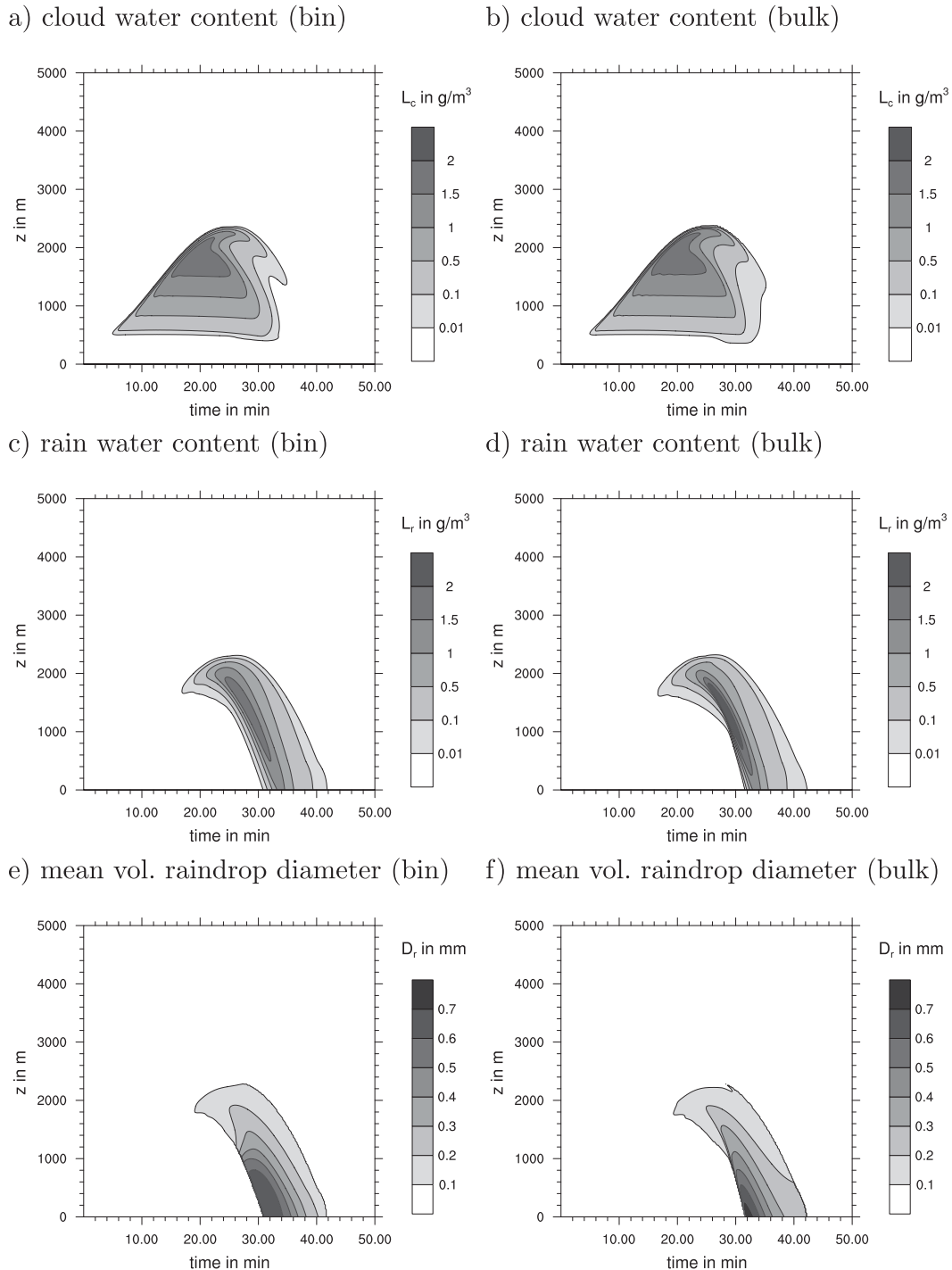


FIG. 1. Time–height diagrams of cloud water content, rainwater content, and mean volume raindrop diameter of the (left) kinematic 1D bin and (right) two-moment bulk microphysics model simulations for $N_a = 100 \text{ cm}^{-3}$, $\Gamma_* = 1.5 \text{ K}$, $w_0 = 2 \text{ m s}^{-1}$, and $\tau_w = 50 \text{ min}$.

the cloud droplets reaches about $40 \mu\text{m}$ at the time of precipitation onset.

The bulk scheme evolves in a manner that both qualitatively and quantitatively captures the behavior of

the much more complex bin microphysical scheme. This is evident in the similarity between the right and left columns in Figs. 1 and 2. The bulk model well represents the height and time at which rain forms, the subsequent

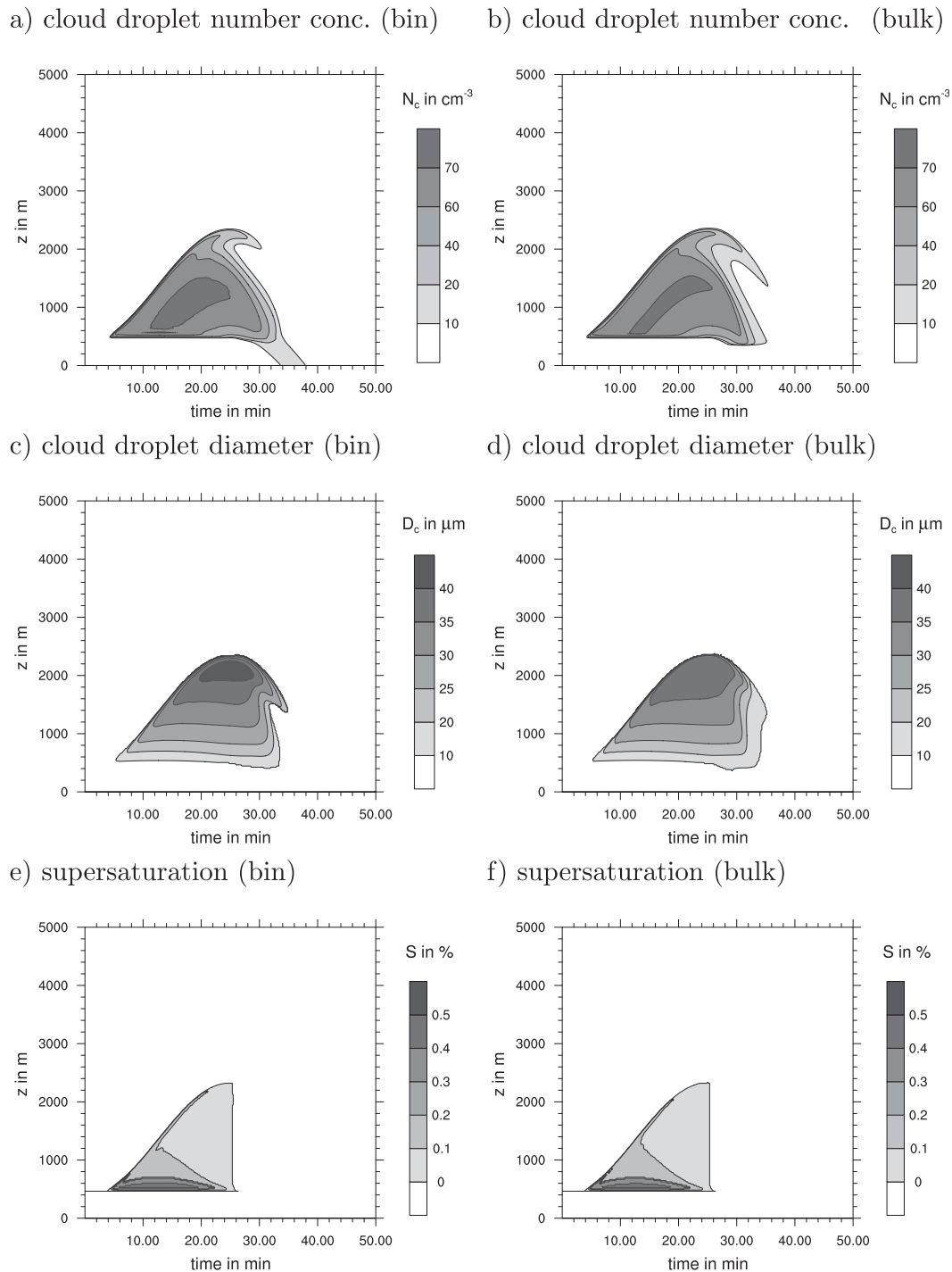


FIG. 2. As in Fig. 1 but showing the cloud droplet number concentration, the mean volume cloud droplet diameter, and the supersaturation.

evolution of the rain shaft, and the structure of the supersaturation field near cloud base. The largest discrepancies are evident in the rainwater content—which is slightly overestimated by the two-moment scheme, probably owing to an overestimation of gravitational sorting

by the nonlinear sedimentation (Wacker and Seifert 2001)—and in the inability to represent cloud droplets within the rain shaft (e.g., Figs. 2a,b).

Overall, the bulk microphysical model describes the evolution of precipitation consistently with the bin

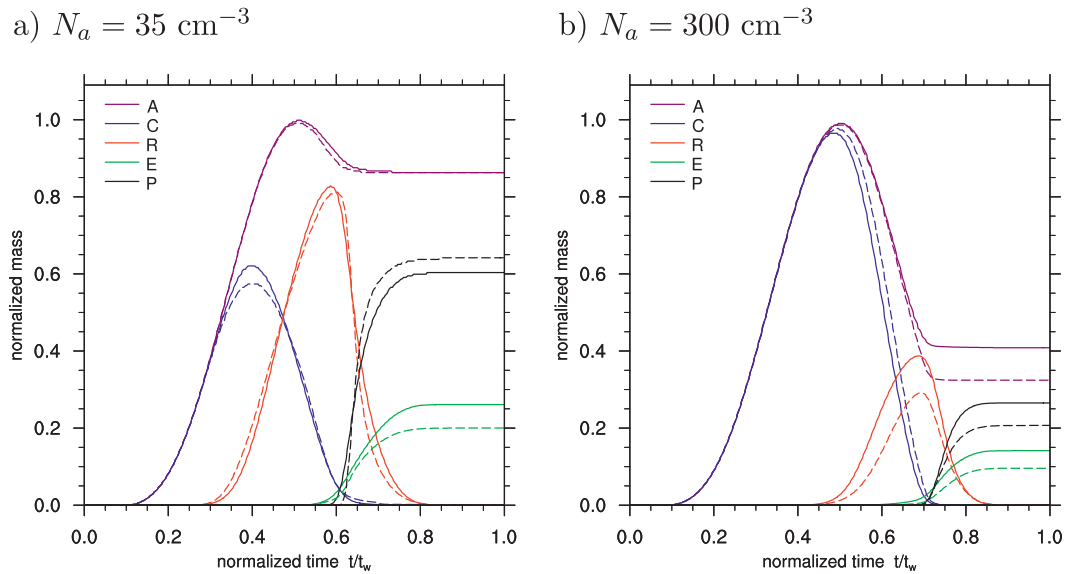


FIG. 3. Normalized time series of the vertically integrated normalized water budget of the 1D cloud model for (a) $N_a = 35 \text{ m}^{-3}$ and (b) $N_a = 300 \text{ m}^{-3}$; both with $\Gamma_* = 1.5 \text{ K}$, $w_0 = 2 \text{ m s}^{-1}$, and $\tau_w = 50 \text{ min}$ (solid lines: bin microphysics, dashed lines: two-moment bulk scheme).

microphysical model. This is demonstrated in Fig. 3, which presents the time-evolving integrated water budget for two cases: the first with $N_a = 35 \text{ cm}^{-3}$ and the second with $N_a = 300 \text{ cm}^{-3}$.

The water budget in Fig. 3 is decomposed as follows:

$$A = C + R + E + P, \quad (17)$$

where A is the available condensate; C , cloud; R , rain-water; E , evaporation; and P , precipitation. The five terms are calculated as follows:

$$C(t) = \frac{1}{\mathcal{M}_w} \int_{z=0}^{\infty} q_c dz, \quad (18)$$

$$R(t) = \frac{1}{\mathcal{M}_w} \int_{z=0}^{\infty} q_r dz, \quad (19)$$

$$A(t) = \frac{1}{\mathcal{M}_w} \int_{z=0}^{\infty} \int_{t=0}^t \left. \frac{\partial q_c}{\partial t} \right|_{\text{cond}} dt' dz, \quad (20)$$

$$E(t) = \frac{1}{\mathcal{M}_w} \int_{z=0}^{\infty} \int_{t=0}^t \left. \frac{\partial q_r}{\partial t} \right|_{\text{eva}} dt' dz, \quad (21)$$

and

$$P(t) = \frac{1}{\mathcal{M}_w} \int_{t=0}^t r_{q,r}(0, t') dt', \quad (22)$$

where $r_{q,r}(0, t)$ denotes the rain rate at the surface. The normalization factor,

$$\mathcal{M}_w = \rho_0 \mathcal{H}^2 \Gamma_l = \frac{c_p}{\pi^2 L_w} \rho_0 w_0^2 \tau_w^2 \Gamma_*, \quad (23)$$

is twice the liquid water path at the time $\tau_w/2$ when the cloud reaches its maximum depth \mathcal{H} . Hence $A(\tau_w/2) = 1$. Here Γ_l is the liquid-water lapse rate; its particular form can be derived by noting that $\mathcal{H} = w_0 \tau_w / \pi$ and $\Gamma_l \simeq (c_p / L_w) \Gamma_*$. The normalized precipitation amount P is identical to the most common definition of the precipitation efficiency as the ratio of surface precipitation to total condensate.

Overall the bulk microphysical model partitions the various components of the available condensed water similarly to the reference (bin) microphysical model. Not only does the bulk model well represent the different times at which rain develops in these two simulations, it also well represents the precipitation efficiency, both at cloud base (which is given by $E + P$) and at the surface.

4. Principal sensitivities

In this section we explore the principal parameter sensitivities of the solutions. To the extent that the bulk-microphysical model can represent the sensitivities of the bin-microphysical model, its analytic tractability provides a framework for developing macroscopic microphysical relationships that could, for instance, be used to parameterize the microphysical evolution on the cloud scale. We focus on three issues: the relationship between the aerosol and mean cloud-droplet number

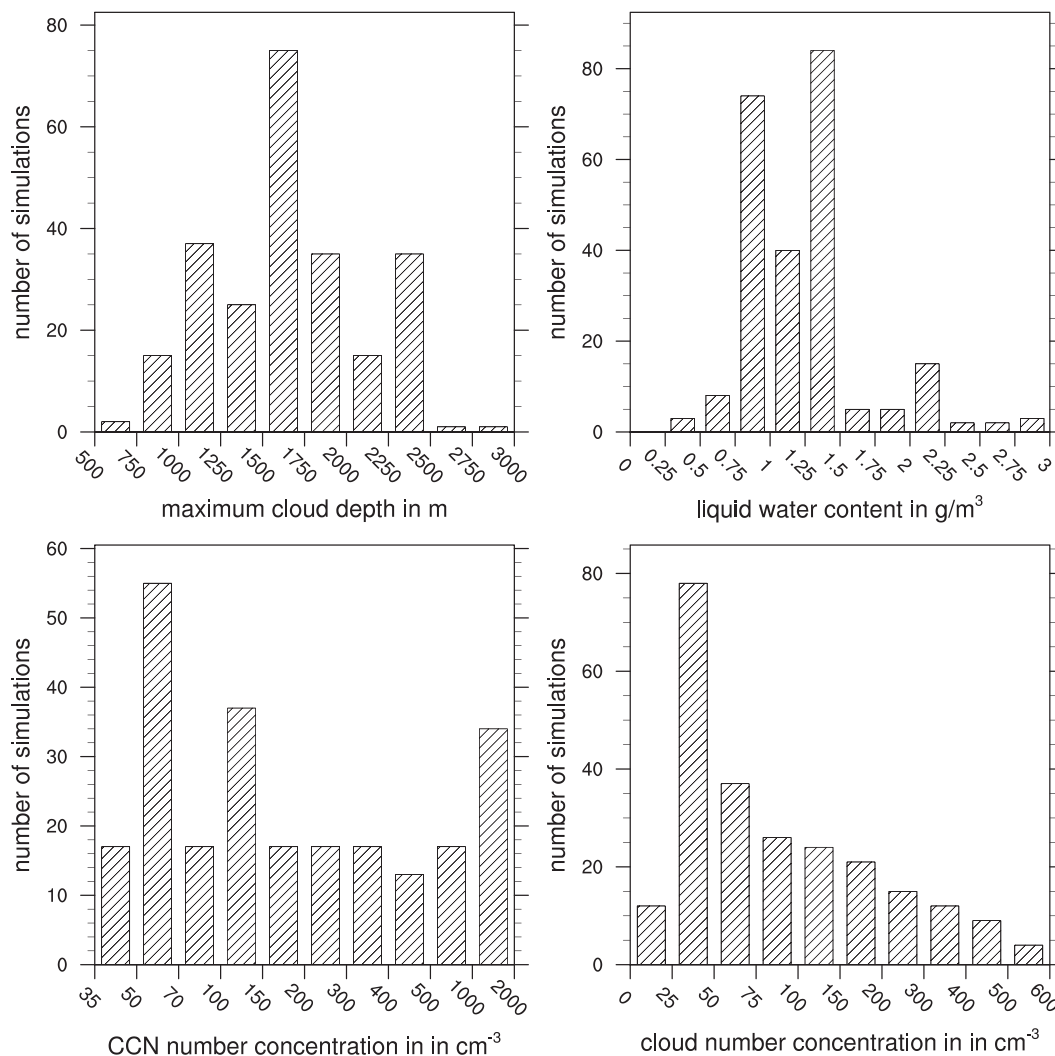


FIG. 4. Histograms of the cloud depth \mathcal{H} (m) and the characteristic liquid water content $\mathcal{L}_0 = M_w/\mathcal{H}$ (g m^{-3}) as well as the assumed CCN number concentration and the resulting cloud droplet concentrations (cm^{-3}) of the 241 simulation of the kinematic 1D model with $w_0 \in [1, 3] \text{ m s}^{-1}$, $\tau_w \in [30, 70] \text{ min}$ and $\Gamma_* \in [0.5, 3] \text{ K km}^{-1}$.

concentration, the autoconversion time scale for the cloud as a whole, and the precipitation efficiency. Our analysis is informed by a great many integrations of the simple model, chosen to sample a characteristic range of the governing parameters. The parameter space sampled by our integrations is characterized in terms of the cloud height \mathcal{H} , the characteristic liquid water content \mathcal{L}_0 , the assumed CCN concentration, and the resulting cloud droplet number concentration with the help of Fig. 4. In the choice of the simulations performed for this study we have attempted to cover the range of typical or plausible parameters for maritime as well as continental shallow cumulus clouds with moderate cloud depth not exceeding 3000 m. The limitation to cloud depths below this value of 3000 m is mainly a restriction of the 1D

model, as its assumptions become increasingly untenable as clouds deepen.

a. A parameterization of activation

The number of cloud droplets is closely related but not equal to the number of CCN (or aerosol particles); therefore, it is desirable to develop a parameterization of the activated fraction N_c/N_a that is at least a function of w_0 and N_a itself. The literature contains a number of proposals for such a parameterization, for example by Ghan et al. (1993) among others. While we do not wish to rule out the applicability of the earlier work, our analysis encourages a slightly different approach.

From the activation scheme used in the two-moment bulk model we can see that the maximum supersaturation

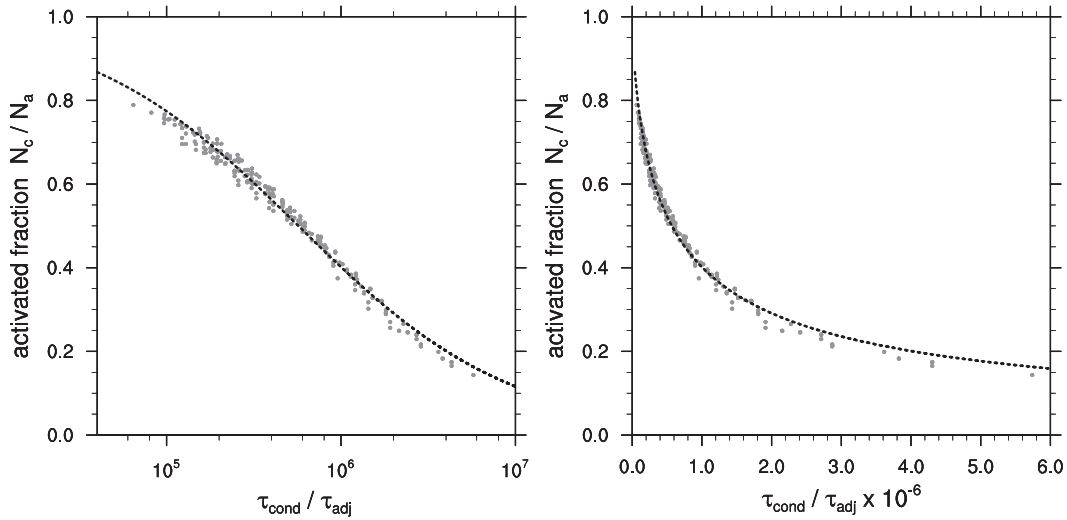


FIG. 5. Scatterplots of the activated fraction \bar{N}_c/N_a as a function of $\tau_{\text{cond}}/\tau_{\text{adj}}$: (left) log scale and (right) linear scale. The dotted line is a least squares fits with $1/(1 + \alpha x^\beta)$.

is the result of two competing processes or time scales: the microscopic condensation-adjustment time scale τ_c [given by Eq. (13)], which describes the growth of the cloud droplets, and the macroscopic condensation time scale $\tau_{\text{cond}} = (w\Gamma_l)^{-1}$, which corresponds to the rate at which excess water vapor is produced by the updraft. Instead of the actual condensation-adjustment time scale, which includes the unknown parameters N_c and \bar{r}_c , we use a potential condensation-adjustment time scale $\tau_{\text{adj}} = (4\pi D_v N_a \bar{r}_{\text{cb}})^{-1}$, which replaces N_c with the total number of CCN and \bar{r}_c with a typical cloud droplet radius r_{cb} near cloud base, which scales with $N_a^{-1/3}$:

$$\bar{r}_{\text{cb}} = r_{\text{ref}} \left(\frac{N_{\text{ref}}}{N_a} \right)^{1/3}, \quad (24)$$

with arbitrarily chosen reference values $r_{\text{ref}} = 5 \mu\text{m}$ and $N_{\text{ref}} = 50 \text{ cm}^{-3}$. If we assume that the number of cloud droplets is only a function of N_a , τ_{adj} , and τ_{cond} , we find that this dimensionally admits only solutions of the form $N_c/N_a = g(\tau_{\text{cond}}/\tau_{\text{adj}})$, where the function g is determined empirically. In terms of our control parameters this dimensionless activation number reads

$$\frac{\tau_{\text{cond}}}{\tau_{\text{adj}}} = \frac{4\pi D_v N_a \bar{r}_{\text{cb}}}{w\Gamma_l} = 4\pi^2 D_v r_{\text{ref}} N_{\text{ref}}^{1/3} \left(\frac{N_a^{2/3} L_v}{c_p \Gamma_* w_0} \right). \quad (25)$$

Figure 5 shows the activated fraction \bar{N}_c/N_a as a function of $\tau_{\text{cond}}/\tau_{\text{adj}}$. Here the cloud droplet concentration \bar{N}_c is averaged vertically in cloud and over the updraft period. The scatterplot shows that $\tau_{\text{cond}}/\tau_{\text{adj}}$ is

able to explain most of the variance of \bar{N}_c/N_a . A possible fit to the data is

$$\begin{aligned} \frac{\bar{N}_c}{N_a} &\cong \frac{1}{1 + \alpha_a (\tau_{\text{cond}}/\tau_{\text{adj}})^{\beta_a}} \\ &= \frac{1}{1 + 8.404 \times 10^{-5} (\tau_{\text{cond}}/\tau_{\text{adj}})^{0.708}}. \end{aligned} \quad (26)$$

In general, we expect α_a and maybe β_a to depend on the properties/composition of the aerosol distribution. In the following we will simply focus only on the dependency of the cloud droplet concentration on N_a , w_0 , and Γ_* .

Finally, we note that, in contradistinction to existing parameterizations of droplet activation, Eq. (25) suggests that the liquid water lapse rate plays a role in setting the activated fraction. In our model, mixing reduces the lapse rate of liquid water at all levels; that is, parcels of cloud base air are not assumed to be adiabatic, hence this term. In fully developed clouds it is not unusual to find nearly adiabatic parcels near cloud base; however, because mixing scales with the cloud size, in the formative stages of a cloud it appears more likely that the liquid water lapse rate would be less than the adiabatic value. Moreover, to the extent one is interested in parameterizing the cloud-averaged cloud-drop concentration, account must be made of the fact that the majority of cloudy updrafts will not have water contents approaching adiabatic values. For both of these reasons we argue that the retention of such an effect (the degree of adiabaticity of the cloud) in the activation scheme

captures more than just artifacts of our particular formulation of the kinematic model.

b. Macroscopic autoconversion time scale

What is the time scale for rain formation in the bulk model, and how does it depend on the kinematic and thermodynamic properties of the cloud? To derive a characteristic time scale for rain formation we start from an even simpler model based on the equation for the cloud water specific humidity q_c with a constant condensation rate τ_{cond}^{-1} given by (cf. Stevens and Seifert 2008)

$$\frac{dq_c}{dt} = \frac{1}{\tau_{\text{cond}}} - k_{\text{au}} q_c^4 N_c^{-2} \phi_{cc}(\epsilon) - k_{cr} q_c q_r \phi_{cr}(\epsilon). \quad (27)$$

Here ϵ is the dimensionless rain fraction

$$\epsilon = \frac{q_r}{l}, \quad (28)$$

where $l = q_r + q_c$ and q_r is the rainwater mixing ratio. The functions

$$\phi_{cc}(\epsilon) = 1 + 600 \frac{\epsilon^p (1 - \epsilon^p)^3}{(1 - \epsilon)^2} \quad (29)$$

with $p = 0.68$ and

$$\phi_{cr}(\epsilon) = \left(\frac{\epsilon}{\epsilon + \kappa} \right)^4 \quad (30)$$

with $\kappa = 5 \times 10^{-4}$ are the universal similarity functions of the SB01 model for autoconversion and accretion, respectively. The autoconversion parameter

$$k_{\text{au}} = \frac{k_{cc} \rho_0^3 (\nu + 2)(\nu + 4)}{20 x^* (\nu + 1)^2} \cong 4.87 \times 10^{18} \text{ s}^{-1} \text{ m}^{-6} \quad (31)$$

depends on the shape parameter ν of the cloud droplet size distribution, here chosen as $\nu = 3$, the separating mass between cloud droplets and raindrops $x^* = 2.6 \times 10^{-10}$ kg (corresponding to an equivalent diameter of about $80 \mu\text{m}$), and the kernel coefficient for autoconversion $k_{cc} = 9.44 \times 10^9 \text{ m}^3 \text{ s}^{-1} \text{ kg}^{-2}$. The kernel coefficient for accretion is $k_{cr} = 4.33 \text{ s}^{-1}$.

The applicability of (27) to the present circumstance requires the specification of the condensation rate. Here we relate it to the average updraft speed in the active phase of cloud development so that

$$\tau_{\text{cond}} \cong (\overline{w} \Gamma_l)^{-1} \cong \left(\frac{w_0}{\pi} \Gamma_l \right)^{-1} = \left(\frac{\rho_0 c_p}{\pi L_v} w_0 \Gamma_* \right)^{-1}. \quad (32)$$

Hence the microphysical spectrum evolves due the combined influence of condensation and kinetic processes.

Following Stevens and Seifert (2008) we define the time τ_* , a measure for the onset of the first in-cloud rain, as a balance of production of cloud water by condensation and its depletion by the collision-coalescence process [cf. Eq. (27) of Stevens and Seifert 2008]:

$$\tau_* = \left[\beta_* + \sqrt{\beta_*^2 + \frac{\tau_0^4}{(1 - \epsilon_*)^4 \phi_{cc}(\epsilon_*)}} \right]^{1/2}, \quad (33)$$

where $\epsilon_* = \epsilon(\tau_*)$ is the rain fraction at time τ_* ,

$$\beta_* = \frac{k_{cr} N_c^2 \tau_{\text{cond}}}{2 k_{\text{au}}} \frac{\epsilon_* \phi_{cr}(\epsilon_*)}{(1 - \epsilon_*)^3 \phi_{cc}(\epsilon_*)}, \quad \text{and} \quad (34)$$

$$\tau_0 = N_c^{1/2} \tau_{\text{cond}}^{3/4} k_{\text{au}}^{-1/4}. \quad (35)$$

We subsequently refer to τ_* as the macrophysical autoconversion time scale. It differs, as a result of microphysical processes, from the bulk time scale τ_{cond} that describes the rate at which the mean volume of cloud droplets increases as a result of condensation during the active phase of the cloud.

Our hypothesis is that the rain efficiency in our cumulus-draft model can be related to the ratio of the macrophysical autoconversion time scale τ_* and the cloud lifetime τ_w . To evaluate τ_* , however, requires knowledge of ϵ_* , the rain fraction at the time when the rate of rain production balances the mean condensation rate. Stevens and Seifert (2008) simply approximated τ_* by τ_0 because

$$\lim_{\epsilon_* \rightarrow 0} \tau_* = \tau_0 \quad (36)$$

amounts to assuming that ϵ_* is small and hence that the aging of the cloud droplet distribution described by ϕ_{cc} can be neglected. For many aspects of the evolution this effect is critical and must be incorporated; therefore, here we endeavor to parameterize ϵ_* .

Noting that $d\epsilon/dt = \tau_{\text{cond}}^{-1}$, it follows from Eqs. (27) and (28) that

$$\frac{d\epsilon}{dt} = \pi_1 (1 - \epsilon)^4 \phi_{cc}(\epsilon) l^3 - \pi_2 \epsilon (1 - \epsilon) \phi_{cr}(\epsilon) l - \frac{\epsilon}{l}, \quad (37)$$

with dimensionless coefficients $\pi_1 = k_{\text{au}} \tau_{\text{cond}} / N_c^2$ and $\pi_2 = k_{cr} \tau_{\text{cond}}$. To calculate a better analytic estimate of the time scale τ_* it would be necessary to solve this highly nonlinear ordinary differential equation from the initial condition $\epsilon(0) = 0$ up to ϵ_* . For large π_1 (small N_c ; i.e., the extremely maritime case) this is actually possible by successive series expansion, but solutions for small π_1

(large N_c) are unfortunately not easily accessible. Therefore we proceed here with a more pragmatic approach. Since the initial condition for ϵ is zero, ϵ_* can only be a function of π_1 and π_2 ; by using numerical solutions of Eq. (37), we find that ϵ_* is only a function of $\pi_1/\pi_2 = k_{\text{au}}/(k_{\text{cr}}^2 N_c^2 \tau_{\text{cond}})$ and can be parameterized by

$$\epsilon_* \approx \epsilon_* = 0.10 \tanh \left[16.135 \left(\frac{k_{\text{au}}}{k_{\text{cr}}^2 N_c^2 \tau_{\text{cond}}} \right)^{3/10} \right], \quad (38)$$

as shown in Fig. 6. This parameterization, together with Eqs. (33)–(35), provides another and hopefully better estimate for the time scale τ_* as it includes (parametrically) the effects of the aging of the cloud droplet size distribution by collision–coalescence. Hereafter we define

$$\tau_{\text{au}} = \frac{1}{3} \tau_*(\epsilon_*'), \quad (39)$$

with ϵ_*' given by (38). The additional factor of $1/3$ is introduced as a tuning factor to account for the fact that Eq. (33) assumes a constant condensation rate, and our draft model admits a temporally evolving rate of condensation.

Another approach to evaluating τ_* is to look for a multivariate power-law ansatz to the numerical solutions, such that

$$\tau_{\text{au}} \approx \tau_0 \pi_1^\alpha \pi_2^\beta. \quad (40)$$

This yields a fit of the form

$$\tau_{\text{au}} \approx \tau_1 = 0.16 N_c^{0.38} \tau_{\text{cond}}^{0.69} k_{\text{au}}^{-0.19} k_{\text{cr}}^{-0.12}. \quad (41)$$

While it turns out that τ_1 provides an inferior approximation to τ_* as compared to Eq. (39), it is analytically more tractable, and will be useful later on, when we interpret the implications of our hypothesis that τ_*/τ_w parameterizes the precipitation efficiency.

In Fig. 7 we compare the estimates for the macroscopic autoconversion time scale with the results of the spectral and the two-moment microphysical simulations. The two-moment simulations agree very well with the results of the spectral model, which supports our choice to use the SB01 approach as a starting point for the investigation. The zeroth-order estimate τ_0 can describe the sensitivities qualitatively but overestimates the dependencies, especially for N_a and Γ_* (a factor already recognized in Stevens and Seifert 2008). The estimate τ_{au} agrees best with the simulations, most markedly in the left panel of Fig. 7, which shows how the time scale for rain formation depends on N_a .

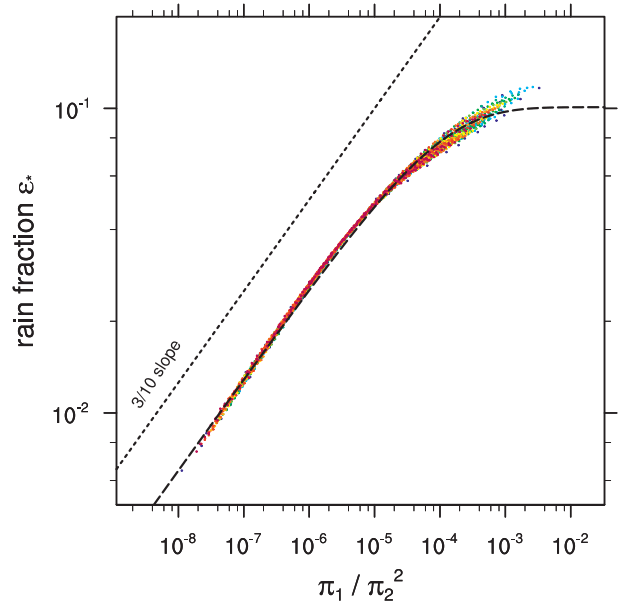


FIG. 6. Scatterplot of the rain fraction ϵ_* at time τ_* from numerical solutions of Eq. (37) for various values of $\pi_1 = k_{\text{au}} \tau_{\text{cond}} / N_c^2$ and $\pi_2 = k_{\text{cr}} \tau_{\text{cond}}$. Also shown is the parameterization of ϵ_* as a function of π_1 / π_2^2 given by Eq. (38).

Differences between our various estimates of τ_* principally reflect the degree to which they incorporate the aging of the cloud droplet size distribution. Such a process accelerates the rain formation and its neglect can lead to significant discrepancies, especially for polluted clouds. This built-in negative feedback is somewhat weaker for the other sensitivities, that is, w_0 and Γ_* , as those do not affect the cloud droplet size distribution as directly as N_a . Nevertheless, this robustness is obviously an important property of the stochastic collection equation that is not taken into account in many simple parameterizations of the warm rain process. Although better than the other estimates, τ_{au} is still too sensitive to N_a . For high w_0 and high Γ_* the analytical estimates also overestimate the speed of rain formation (Fig. 7) but differ less sharply from one another. The deviations of τ_* from the reference model likely reflect the use of the time-averaged condensation rate in τ_{cond} instead of solving the fully time-dependent problem.

c. Precipitation within a finite cloud lifetime

1) THE PRECIPITATION THRESHOLD

It indeed turns out that for the type of clouds modeled here, τ_{au}/τ_w is a good measure of whether precipitation develops. Figure 8 shows a scatterplot of the precipitation efficiency as a function of $\tau_{\text{updraft}}/\tau_{\text{au}}$, with $\tau_{\text{updraft}} = \tau_w/2$. For this idealized 1D model all clouds with $\tau_{\text{updraft}}/\tau_{\text{au}} > 1$ precipitate, whereas clouds with a smaller ratio of those

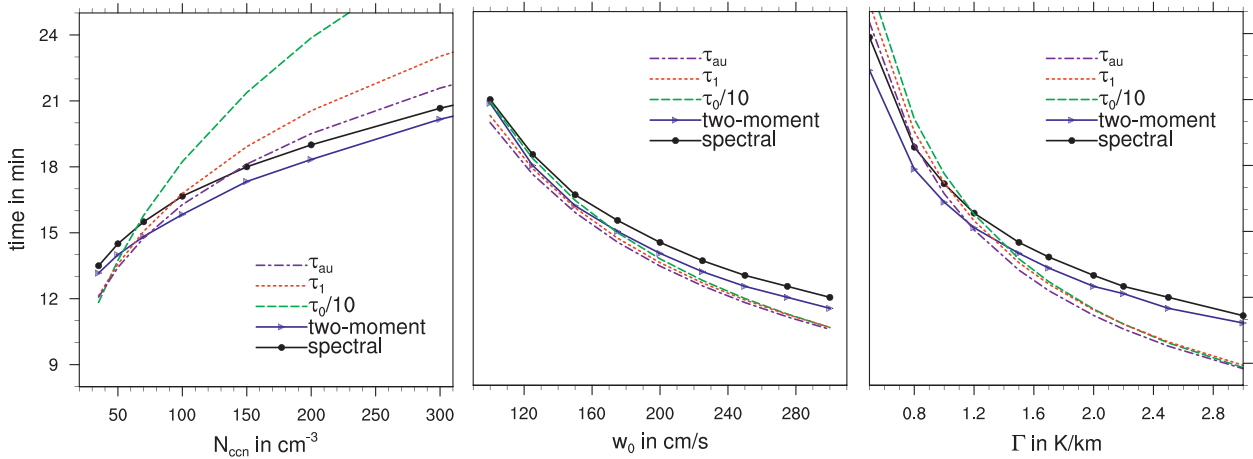


FIG. 7. Time of first in-cloud rain ($\mathcal{M}_w R > 10^{-4} g cm^{-2}$) as a measure of the macroscopic autoconversion time scale as function of (left) N_a for $w_0 = 2 m s^{-1}$, $\Gamma_* = 1.5 K km^{-1}$; (middle) the maximum vertical velocity w_0 for $N_a = 50 cm^{-3}$, $\Gamma_* = 1.5 K km^{-1}$; and (right) the lapse rate Γ_* for $N_a = 50 cm^{-3}$, $w_0 = 2 m s^{-1}$. All simulations with $\tau_w = 50 min$. The τ_0 , τ_1 , and τ_{au} are analytical estimates of the autoconversion time scale τ_* (plotted is $\tau_0/10$).

two time scales do not precipitate. For large $\tau_{updraft}/\tau_{au}$ the precipitation efficiency increases but shows considerable scatter, especially at the surface. On one hand, this very clear and simple behavior of this model might be partly a result of necessary simplifications. For example, the downdraft is as strong as the updraft and affects all cloud parcels. This might be one reason for the clear threshold behavior with respect to $\tau_{updraft}/\tau_{au}$. On the other hand, our findings—for instance, that clouds only precipitate when large cloud droplets develop in an updraft (or active cloud) with sufficient cloud water content that allows further growth by accretion—are consistent with the recent observational results of Burnet and Brenguier (2008) based on in situ measurements in

shallow cumuli during the Small Cumulus Microphysics Study in Florida.

Although not unexpected, it is interesting to see that the finite cloud lifetime leads to some kind of a threshold behavior of the precipitation formation. This is especially interesting as Kessler (1969) in his original publication of his threshold-based autoconversion rate motivates the threshold behavior intuitively with a macroscopic cloud, not with microphysical processes:

As we know, water clouds sometimes persist for a long time without evidence of precipitation, but various measurements show that cloud amounts $>1 g/m^3$ are usually associated with production of precipitation. It

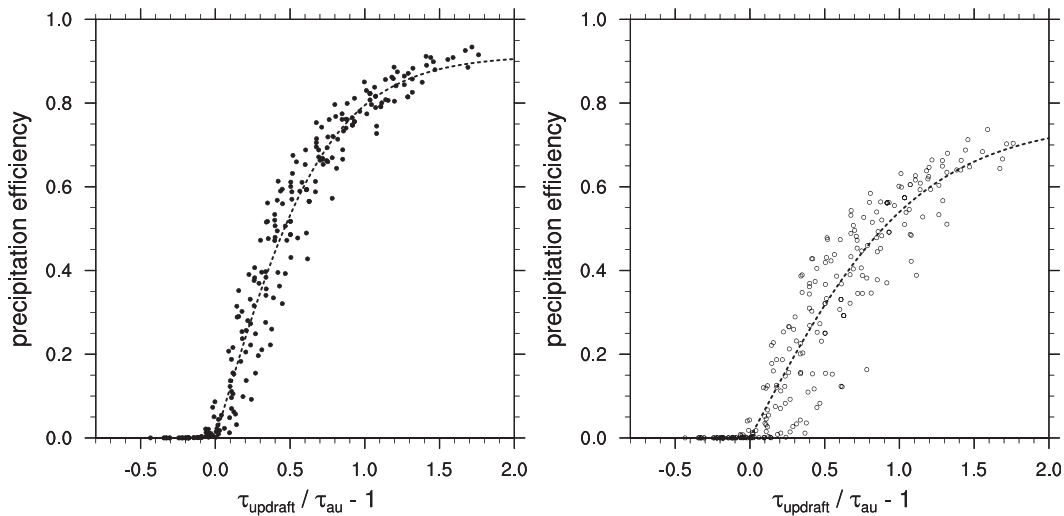


FIG. 8. Scatterplot of the precipitation efficiency at (left) a virtual cloud base, $P + E$, and (right) at the surface, P , as a function of $\tau_{updraft}/\tau_{au}$.

seems reasonable to model nature in a system where the rate of cloud autoconversion increases with the cloud content but is zero for amounts below some threshold (Kessler 1969, p. 26).

Because Kessler used the liquid water content as the threshold parameter, it is interesting to see how the threshold that we have developed in terms of time scales can be reformulated in terms of a characteristic liquid water content of the cloud. Using $\mathcal{L}_0 = \mathcal{M}_w/\mathcal{H} = \rho_0\tau_w/\tau_{\text{cond}}$ and, for simplicity, τ_1 instead of τ_{au} , we find that $\tau_{\text{updraft}}/\tau_{\text{au}} > 1$ is equivalent to

$$\mathcal{L}_0 > \mathcal{L}_* \cong 0.2\rho_0 N_c^{0.55} \tau_w^{-0.45} k_{\text{au}}^{-0.27} k_{\text{cr}}^{-0.18}. \quad (42)$$

This liquid water threshold \mathcal{L}_* is shown in Fig. 9. Note that it differs from a critical size parameterization as the latter would yield a liquid water threshold dependent on N_c . The somewhat weaker dependence on N_c in (42) implies that, if precipitation thresholds are to be interpreted in terms of a critical radius (Gerber 1996), this radius must have a very weak dependence on both the mean droplet size and other microphysical parameters. For low cloud droplet number concentrations, that is, 20–100 cm^{-3} , the liquid water threshold (42) has values of 0.2–1.0 g m^{-3} , which also agrees with the autoconversion thresholds that are typically chosen in mesoscale models. This interpretation of Kessler's autoconversion threshold is intuitively reasonable and, as we have shown, consistent with the fact that the SCE itself does not show any threshold behavior. Nevertheless, it is obviously very different from other interpretations (e.g., Liu and Daum 2004).

Instead of using τ_{updraft} , τ_w , or \mathcal{L}_0 as the threshold parameter, one could also attempt to use the cloud depth \mathcal{H} , which has sometimes been used to stratify observations of trade wind cumuli with regard to in-cloud radar echoes (see, e.g., Byers and Hall 1955; Snodgrass et al. 2009). Unfortunately, in this case one would have to make additional assumptions about w_0 and Γ_* , which are usually not measured. Therefore we postpone such a comparison with measurements of the onset of precipitation to the future.

2) A PARAMETERIZATION OF THE PRECIPITATION EFFICIENCY OF SHALLOW CUMULUS CLOUDS

As shown in Fig. 8, the precipitation efficiency increases for smaller autoconversion time scales with $\tau_{\text{updraft}}/\tau_{\text{au}} > 1$ but shows a lot of scatter, especially for low precipitation efficiencies. The reason is that for clouds with little liquid water the whole rain formation process will be very slow; that is, although those clouds start to produce some raindrops at $\tau_{\text{updraft}}/\tau_{\text{au}} \cong 1$, they are very inefficient in producing more rain, for example,

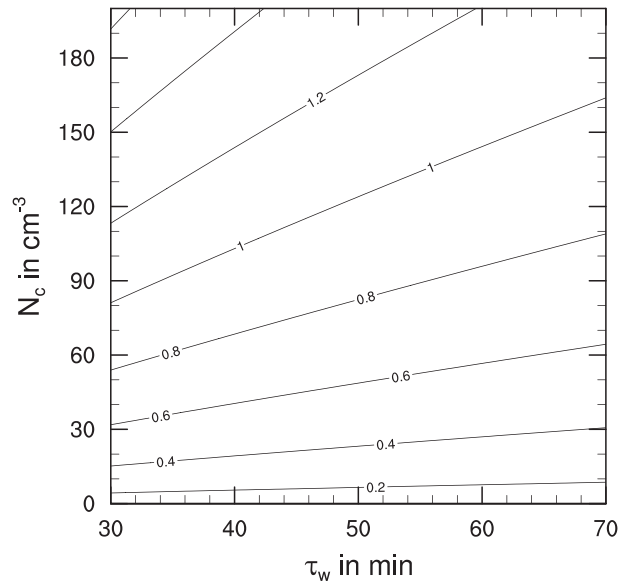


FIG. 9. Liquid water threshold \mathcal{L}_* (g m^{-3}) for precipitation formation in cumulus clouds as a function of the cloud droplet number concentration N_c and the cloud lifetime τ_w .

by accretion. From Srivastava (1988) and SB01 we know that the time scale of the whole collision–coalescence process scales with the mass of the available liquid water. This motivates us to use

$$\chi = \left(\frac{\tau_{\text{updraft}}}{\tau_{\text{au}}} - 1 \right) \frac{\mathcal{M}_w}{\mathcal{M}_{\text{ref}}}, \quad (43)$$

with an arbitrarily chosen reference value $\mathcal{M}_{\text{ref}} = 1 \text{ kg m}^{-2}$ as a predictor of the precipitation efficiency. This can be seen as a dimensionless time scale describing the rain formation for $\tau_{\text{updraft}}/\tau_{\text{au}} > 1$. The same data for the surface precipitation efficiency as in Fig. 8 is shown in Fig. 10 and here the data for the low precipitation efficiencies line up slightly better. For small χ the precipitation efficiency shows a linear increase and saturates for larger χ to a constant upper limit. The high precipitation efficiency for large χ might be an artifact of the 1D model, which allows the raindrops to collect all cloud droplets below them. Therefore the results for large χ (i.e., precipitation efficiencies larger than 40%) should be interpreted with caution. A parameterization of cloud-base and surface precipitation efficiency for $\tau_{\text{updraft}}/\tau_{\text{au}} > 1$ is

$$P_{\text{cb}} \approx 0.91 \tanh \left[1.33 \left(\frac{\tau_{\text{updraft}}}{\tau_{\text{au}}} - 1 \right) \right] \quad (44)$$

and

$$P \approx 0.65 \tanh \left[5.49 \left(\frac{\tau_{\text{updraft}}}{\tau_{\text{au}}} - 1 \right) \frac{\mathcal{M}_w}{\mathcal{M}_{\text{ref}}} \right]. \quad (45)$$

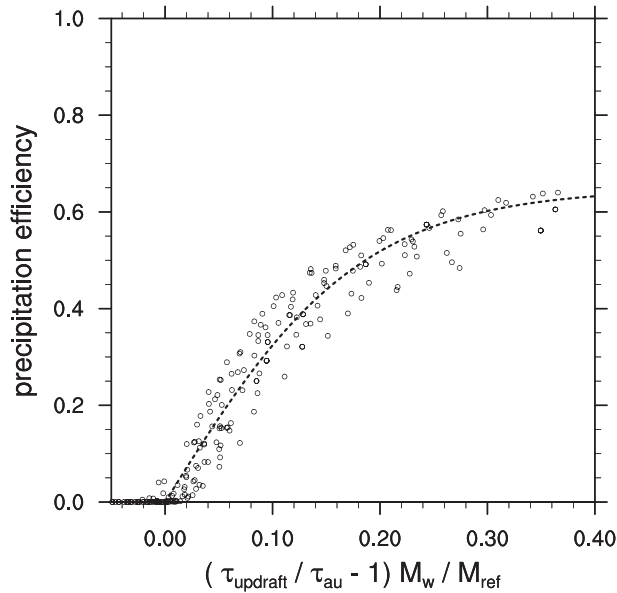


FIG. 10. Scatterplot of the precipitation efficiency at the surface as a function of $\chi = (\tau_{\text{updraft}}/\tau_{\text{au}} - 1)M_w/M_{\text{ref}}$.

The surface precipitation efficiency P will in general also depend on the cloud-base height and the surface temperature, but both dependencies have not been investigated here. Instead of using the scaling with M_w for the precipitation efficiency as has been done here, it would also be possible to combine the cloud-base efficiency, given by Eq. (44), with a parameterization of the below-cloud evaporation (e.g., following Feingold 1993). To extend these ideas to fields of clouds one would need an explicit probability density function of cloud heights over which Eqs. (44) and (45) could then be integrated.

5. Summary and conclusions

We have presented a theoretical approach describing the rain formation in small isolated cumulus clouds. Our approach provides a link between the microphysical processes such as activation, collision-coalescence, etc. and the macroscopic forcing by updraft velocity and the cloud thermodynamical evolution. This framework enables us to explore the interplay among microphysical processes, dynamical forcing, and the lifetime of the cloud. To quantify the evolution of the cloud we utilize spectral and two-moment bulk microphysical models. Within the limitations of the 1D model, and after tuning some parameters such as spectral width, which cannot be predicted by the two-moment scheme, a reasonable agreement is achieved between both modeling approaches. The analysis of both microphysical models leads us to a parameterization of the activation process in terms of the ratio of the (macroscopic) condensation

time scale and a microscopic condensation-adjustment (phase relaxation) time scale. Our main finding is that the precipitation efficiency of the cloud is only a function of the cloud lifetime and a macroscopic autoconversion time scale, where the latter can be derived from the two-moment warm rain scheme. This analysis shows that for a finite-lifetime cloud the aerosol-cloud-precipitation effects are much weaker than expected from a purely microphysical point of view. This robustness is caused by two processes: 1) the aging of the cloud droplet size distribution during the lifetime of the cloud and 2) the importance of accretion for growth of the drizzle-sized drops to larger raindrops. The latter process, especially in combination with the aging effect, is relatively insensitive to CCN variations.

We have shown that the ability of a macroscopic cloud to produce precipitation is determined primarily by two time scales: the autoconversion time scale describing the time needed to produce rain by collision-coalescence in a cloud whose active phase consists of continuous condensation, and the lifetime of the cloud itself. This statement by itself sounds almost trivial, but the difficulties are in specifying each of these time scales. For shallow clouds we assume that the dynamical time scale is dominated by the driving boundary layer processes. At least for this kind of forced shallow cumulus clouds our approach naturally lends itself to the representation of cumulus ensembles, that is, describing the precipitation efficiency of an ensemble of clouds by their joint probability density function of updraft velocity, local lapse rate, and cloud lifetime. Insofar as the individual clouds are not strongly interacting, such an approach would provide a rational framework for linking precipitation formation on large scales with the microphysical processes occurring on the smallest scales, and would be interesting to test, say with LES. In the more general case when the feedbacks of clouds on the dynamics and the interaction between clouds are important, the microphysical time scales approach might still be helpful, but then a more elaborate treatment of the dynamical-microphysical feedbacks would be crucial. The latter would have to be done in terms of the joint PDF of the relevant parameters.

On one hand, the modeling results presented here do have many limitations. Foremost are the simplicity and constraints of the 1D kinematic model, for example, the simplifications in representing entrainment, mixing, and the broadening of the droplet size distribution. On the other, recent analysis of shallow convective clouds and their life cycles based on LES by Heus et al. (2009) suggests that our idealized view might be justified to some extent; for example, their mass flux composite shows a cloud evolution that is strikingly similar to our

simple 1D model. Even the pulsating growth that they found to be present in many clouds could be incorporated into the 1D model, and (here we speculate) maybe it is actually the updraft pulses that define the relevant dynamical and microphysical time scales that support or constrain the formation of rain. In this way, by relating the time scales to the internal dynamics of clouds, our approach could possibly be applied to clouds that exhibit a much more complicated structure and time evolution than our simplistic kinematic 1D model.

Acknowledgments. We thank the two anonymous reviewers and the editor for their comments that helped improve the paper.

REFERENCES

- Beard, K. V., 1976: Terminal velocity and shape of cloud and precipitation drops aloft. *J. Atmos. Sci.*, **33**, 851–864.
- Beheng, K. D., 1994: A parameterization of warm cloud microphysical conversion processes. *Atmos. Res.*, **33**, 193–206.
- , and G. Doms, 1986: A general formulation of collection rates of cloud and raindrops using the kinetic equation and comparison with parameterizations. *Contrib. Atmos. Phys.*, **59**, 66–84.
- Berry, E. X., and R. L. Reinhardt, 1974: An analysis of cloud drop growth by collection. Part II: Single initial distributions. *J. Atmos. Sci.*, **31**, 1825–1831.
- Brenguier, J.-L., 1991: Parameterization of the condensation process: A theoretical approach. *J. Atmos. Sci.*, **48**, 264–282.
- Burnet, F., and J.-L. Brenguier, 2008: Entrainment and mixing in warm convective clouds: effects on droplet spectra and on the onset of precipitation. *Proc. 15th Int. Conf. on Clouds and Precipitation*, Cancun, Mexico, ICCP, 1.7.
- Byers, H. R., and R. K. Hall, 1955: A census of cumulus-cloud height versus precipitation in the vicinity of Puerto Rico during the winter and spring of 1953–1954. *J. Meteor.*, **12**, 176–178.
- Clark, T. L., 1974: A study in cloud phase parameterization using the gamma distribution. *J. Atmos. Sci.*, **31**, 142–155.
- Feingold, G., 1993: Parameterization of the evaporation of rainfall for use in general circulation models. *J. Atmos. Sci.*, **50**, 3454–3467.
- Gerber, H., 1996: Microphysics of marine stratocumulus clouds with two drizzle modes. *J. Atmos. Sci.*, **53**, 1649–1662.
- Ghan, S. J., C. C. Chuang, and J. E. Penner, 1993: A parameterization of cloud droplet nucleation Part I: Single aerosol type. *Atmos. Res.*, **30**, 197–221.
- Gillespie, D. T., 1972: The stochastic coalescence model for cloud droplet growth. *J. Atmos. Sci.*, **29**, 1496–1510.
- Heus, T., H. J. J. Jonker, H. E. A. Van den Akker, E. J. Griffith, M. Koutek, and F. H. Post, 2009: A statistical approach to the life cycle analysis of cumulus clouds selected in a virtual reality environment. *J. Geophys. Res.*, **114**, D06208, doi:10.1029/2008JD010917.
- Kessler, E., 1969: *On the Distribution and Continuity of Water Substance in Atmospheric Circulations*. *Meteor. Monogr.*, No. 32, Amer. Meteor. Soc., 84 pp.
- Khairoutdinov, M., and Y. Kogan, 2000: A new cloud physics parameterization in a large-eddy simulation model of marine stratocumulus. *Mon. Wea. Rev.*, **128**, 229–243.
- Khvorostyanov, V. I., and J. A. Curry, 2006: Aerosol size spectra and CCN activity spectra: Reconciling the lognormal, algebraic, and power laws. *J. Geophys. Res.*, **111**, D12202, doi:10.1029/2005JD006532.
- Liu, Y., and P. H. Daum, 2004: Parameterization of the autoconversion process. Part I: Analytical formulation of the Kessler-type parameterizations. *J. Atmos. Sci.*, **61**, 1539–1548.
- Lohmann, U., and E. Roeckner, 1996: Design and performance of a new cloud microphysics scheme developed for the ECHAM general circulation model. *Climate Dyn.*, **12**, 557–572.
- Lüpkes, C., K. D. Beheng, and G. Doms, 1989: A parameterization scheme for simulating collision/coalescence of water drops. *Contrib. Atmos. Phys.*, **62**, 289–306.
- Milbrandt, J., and M. Yau, 2005a: A multimoment bulk microphysics parameterization. Part I: Analysis of the role of the spectral shape parameter. *J. Atmos. Sci.*, **62**, 3051–3064.
- , and —, 2005b: A multimoment bulk microphysics parameterization. Part II: A proposed three-moment closure and scheme description. *J. Atmos. Sci.*, **62**, 3065–3081.
- Morrison, H., and W. Grabowski, 2007: Comparison of bulk and bin warm rain microphysics models using a kinematic framework. *J. Atmos. Sci.*, **64**, 2839–2861.
- Müller, H., 1928: Zur allgemeinen Theorie der raschen Koagulation. *Kolloidchem. Beihefte*, **27**, 223–250.
- Pruppacher, H. R., and J. D. Klett, 1997: *Microphysics of Clouds and Precipitation*. 2nd ed. Kluwer Academic, 954 pp.
- Reisner, J., R. M. Rasmussen, and R. T. Bruintjes, 1998: Explicit forecasting of supercooled liquid water in winter storms using the MM5 mesoscale model. *Quart. J. Roy. Meteor. Soc.*, **124**, 1071–1107.
- Rotstain, L. D., 2000: On the “tuning” of autoconversion parameterizations in climate models. *J. Geophys. Res.*, **105**, 15 495–15 507.
- Seifert, A., 2008: On the parameterization of evaporation of raindrops as simulated by a one-dimensional rainshaft model. *J. Atmos. Sci.*, **65**, 3608–3619.
- , and K. D. Beheng, 2001: A double-moment parameterization for simulating autoconversion, accretion, and self-collection. *Atmos. Res.*, **59–60**, 265–281.
- , A. Khain, U. Blahak, and K. D. Beheng, 2005: Possible effects of collisional breakup on mixed-phase deep convection simulated by a spectral (bin) cloud model. *J. Atmos. Sci.*, **62**, 1917–1931.
- Snodgrass, E. R., L. D. Girolamo, and R. M. Rauber, 2009: Precipitation characteristics of trade wind clouds during RICO derived from radar, satellite, and aircraft measurements. *J. Appl. Meteor.*, **48**, 464–483.
- Srivastava, R., 1988: On the scaling of equations governing the evolution of raindrop size distributions. *J. Atmos. Sci.*, **45**, 1091–1092.
- Stevens, B., and A. Seifert, 2008: Understanding macrophysical outcomes of microphysical choices in simulations of shallow cumulus convection. *J. Meteor. Soc. Japan*, **86**, 143–162.
- von der Emde, K., and U. Wacker, 1993: Comments on the relationship between aerosol spectra, equilibrium drop size spectra, and CCN spectra. *Contrib. Atmos. Phys.*, **66**, 157–162.
- von Smoluchowski, M., 1916: Drei Vorträge über Diffusion, Brownsche Molekularbewegung und Koagulation von Kolloidteilchen. *Physik. Zeitschr.*, **17**, 557–599.
- , 1917: Versuch einer mathematischen Theorie der Koagulationskinetik kolloidaler Lösungen. *Z. Phys. Chem.*, **92**, 129–168.
- Wacker, U., and A. Seifert, 2001: Evolution of rain water profiles resulting from pure sedimentation: Spectral vs. parameterized description. *Atmos. Res.*, **58**, 19–39.